Deposition Study of Indium Trisguanidinate as a Possible Indium Nitride Precursor

Polla Rouf[a], Nathan J. O'Brien[a], Sydney C. Buttera[b], Sean T. Barry[b], Henrik Pedersen[a]

[a] Department of Physics, Chemistry and Biology, Linköping University, SE-58183 Linköping, Sweden

[b] Department of Chemistry, Carleton University, 1125 Colonel By Drive, Ottawa, Ontario K1S 5B6, Canada

[a)] Electronic mail: polla.rouf@liu.se

A time-resolved chemical vapor deposition process for indium nitride (InN) is reported using tris-*N*,*N*-dimethyl-*N*',*N*''-diisopropylguanidinatoindium(III) (**1**) and ammonia plasma at 200 °C. The deposition was self-limiting with respect to the pulse time of **1**, indicative of a surface-controlled deposition chemistry. The films were confirmed to be InN by X-ray photoelectron spectroscopy (XPS) and film thicknesses of 10 nm were measured by X-ray reflectivity (XRR), corresponding to a deposition rate of 0.1 nm/cycle. Grazing incidence X-ray diffraction (GIXRD) showed a hexagonal polycrystalline film with a preferred (002) orientation. Morphology studies suggest an island growth mode. The poor thermal stability of **1**, previously discussed in the literature, prevented full characterization of the deposition process and the deposition of thicker films. It is concluded that while **1** can act as an In precursor for InN, its poor thermal stability prevents its practical use.

I. INTRODUCTION

The high electron saturation velocity, small effective electron mass and high electron mobility of indium nitride (InN)[1,2,3] makes it a suitable material for high frequency electronics. The possibility to integrate InN in existing high electron mobility transistors (HEMTs), currently based on other group 13 nitrides - aluminum nitride (AlN), gallium nitride (GaN) and their alloys, makes InN a key material for future high frequency transistors. However, InN decomposes to In metal and N_2 gas at around 500 °C,[4] making deposition of InN films challenging with conventional methods. Chemical vapor deposition (CVD) routes to InN typically use trimethyl indium ($In(CH_3)_3$) and ammonia (NH_3) as precursors. The low upper temperature tolerated by the InN crystal and the poor thermal reactivity of NH_3 forces InN CVD to use $NH_3/In(CH_3)_3$ in ratios in the order of 100000.[5,6] Rather than relying on gas phase reactivity to form more reactive species, a surface controlled CVD approach with time-resolved precursor delivery could be an alternative way to eliminate the high N/In precursor ratios; such an approach would rely on surface chemical reactions between gas phase species and chemisorbed surface moieties. If self-limiting surface chemistry is achieved, such an approach would be an atomic layer deposition (ALD) process. ALD of InN has been demonstrated using $In(CH_3)_3$ and N_2 plasmas, affording InN of high crystalline quality.[7,8] A successful ALD process for electronic grade InN must produce films with very low impurity levels, particularly for carbon and oxygen; low temperature ALD processes based on precursors with metal-carbon bonds are known to render carbon impurities in the few atomic percent range.[9] It has been shown that plasma ALD of InN requires very long plasma exposures (on the order of 100 s) to reduce the carbon content down to approximately 3 atomic

percent,[8] which demonstrates the importance of designing new In-precursors without In-C bonds or oxygen atoms as constituents. We have previously studied the thermal properties of one such molecule; tris-*N*,*N*-dimethyl-*N*',*N*"-diisopropylguanidinatoindium(III) (**1**, Fig. 1),[10] which has been shown to function as both a CVD precursor[11] and an ALD precursor[12] for deposition of In_2O_3. While previous deposition studies have shown that **1** could be a possible candidate for InN formation, we found by solution phase nuclear magnetic resonance spectroscopy and computational modeling that it degrades upon heating. It was found that degradation of **1** proceeds by a series of diisopropylcarbodiimide de-insertions to form a non-volatile indium compound.[10] Here, we present deposition studies using **1** together with NH_3 plasma in an ALD process to show that **1** can be used to produce InN films. We also confirm the thermal instability of **1** in the bubbler, ultimately demonstrating it to be a non-ideal precursor for this process.

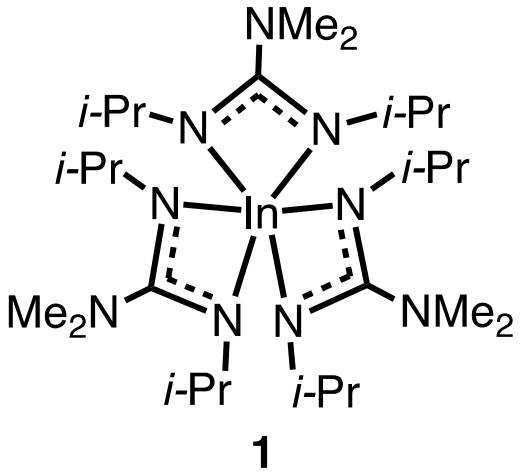

1

FIG. 1. Previously studied precursor tris-*N*,*N*-dimethyl-*N*',*N*"-diisopropylguanidinatoindium(III) **1.**

II. EXPERIMENTAL

A. Film deposition

The deposition of films was carried out in a hot-walled ALD system, Picosun R-200, equipped with a Litmas remote plasma source operating at a pressure of 7 mbar and a continuous flow of N_2 (99.999%) in the reaction chamber. It should be noted that in previously reported CVD and ALD studies of **1**,[11,12] the precursor was placed in an open boat bubbler within a tube furnace-based reactor setup, with the main gas flow aiding the transport of the precursor. In our deposition system, a traditional stainless-steel bubbler container without a dip-tube for the incoming carrier gas was used. Approximately 0.5 g of **1** was placed in a glass vial within the stainless-steel bubbler which was heated to 160 °C. To move **1** into the deposition chamber, a fill-empty pulsing scheme, illustrated in Fig. 2, was necessary due to the low vapor pressure of **1**.

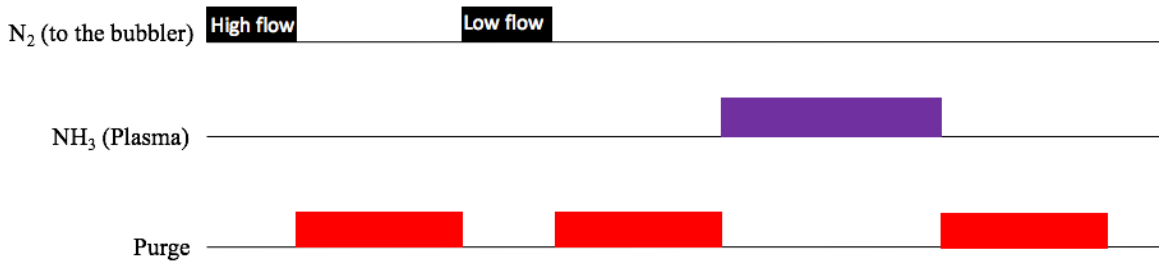

FIG. 2. The pulsing scheme for ALD of InN using **1**.

In the fill-empty pulsing, the bubbler valve was first opened with a high flow (500 sccm) of N_2 through the bubbler for 5 s, where the high flow rate of N_2 slightly increase the pressure in the bubbler, creating a small pressure gradient between the bubbler and the

chamber. This is denoted as the fill sub-pulse. The bubbler was then closed for 10 s to allow mixing of N_2 with the vapor of **1**. The bubbler valve was then opened again but now with a low flow (100 sccm) of N_2, the pressure gradient created in the fill sub-pulse then aided the movement of the precursor into the deposition chamber. This is denoted as the empty sub-pulse. The time for which the bubbler was opened to the chamber during the empty sub-pulse was regarded as the pulse time for **1**. An Ar/NH_3 (100/10 sccm) gas mixture was used to form an NH_3 plasma (the nitrogen source for the film) with a plasma power of 1000 W. The InN deposition was conducted at 200 °C using a cycle sequence with the fill-empty pulse of **1**, 10 s N_2 purge, 13 s NH_3 plasma and 10 s purge (Fig. 2). The films were deposited on Si (001), cut into approximately 15 x 15 mm^2 pieces and used without further surface cleaning.

B. Precursor synthesis

Synthesis of **1** followed the route previously described in the literature.[10,11] Briefly, lithiated guanidinate was synthesized by slowly adding a -35 °C solution of *N*,*N*'-diisopropylcarbodiimide (6.0 g, 47.6 mmol) in Et_2O (20 mL) to a suspension of lithium dimethylamide (2.42 g, 47.6 mmol) in Et_2O (30 mL) at -35 °C. After 3 hours, this mixture was added to a solution of indium trichloride (3.5 g, 15.8 mmol) in THF (30 mL) and stirred for 16 hours. The reaction mixture was concentrated under reduced pressured and the resulting solid dissolved in hexanes, filtered and concentrated to obtain **1**. All synthesis was performed under an inert atmosphere using a N_2-filled GS Glovebox-System (GS081017).

C. Film characterization

The crystallinity of the deposited films was studied using grazing incidence X-ray diffraction (GIXRD) in a PANalytical EMPYREAN MRD XRD with a Cu-anode x-ray tube and 5-axis (x-y-z-v-u) sample stage. PANalytical X'Pert PRO with a Cu-anode tube and Bragg-Brentano HD optics was used in x-ray reflectivity (XRR) mode to measure the thickness of the films. From the XRR measurements, the Kiessig Fringes were used to calculate the thickness of the films using the linearized Bragg's modified law. A LEO 1550 scanning electron microscope (SEM) with an acceleration energy of 20 kV was used to characterize the morphology of the film. The chemical bonding environments in the film were characterized using a Kratos AXIS Ultra DLD X-ray photoelectron spectroscopy (XPS) equipped with an Ar sputtering source. Gaussian-Laurentius (GL (30)) functions were used to fit the experimental XPS data.

III. Results and Discussion

Initial experiments to test the feasibility of **1** as an In precursor for the deposition of InN were undertaken using a solution of 0.5 g of **1** in toluene. Upon bubbling NH_3 (g) through the solution at room temperature, the resultant mixture became cloudy. When the cloudy suspension was allowed to settle and the white precipitate was recovered by filtration (Fig. S1). The precipitate was found to be amorphous by XRD, while XPS of the nitrogen region showed a N 1s peak that could be fitted with a significant In-N contribution (Fig. S2). Initial deposition studies using a 2800 W N_2 plasma and a 250 °C substrate temperature afforded XRD amorphous films where the XPS surface analysis of the N 1s region showed only condensed **1** on the surface. Sputter cleaning of the film revealed a

double peak attributed to condensed **1** and In-N (Fig. S3). After these initial promising results, we undertook deposition studies with NH_3 plasma. Figure 3 shows the saturation curve for the pulse time of **1** while the pulse times for NH_3 plasma (13s) and purges (10s) were kept constant. When the empty sub-pulse time for **1** was 4 s or longer, the growth per cycle was shown to saturate, indicating a self-limiting deposition behaviour.

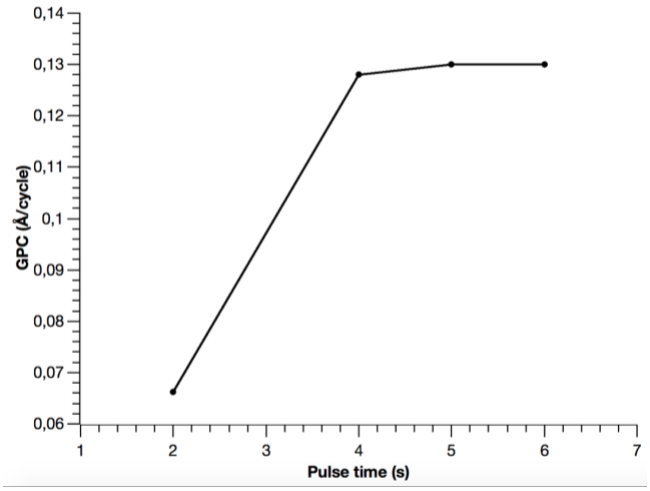

FIG. 3. Saturation curve of precursor **1** under constant conditions of a 13 s NH_3 plasma and 10 s nitrogen purges.

The XRR measurements showed that approximately 10 nm of film was deposited after 800 cycles using an empty sub-pulse time of 5 s for **1** (Fig. 3) on a Si (001) substrate. The GIXRD pattern (Fig. 4) showed polycrystalline, hexagonal InN with a preferred orientation of (002), which was demonstrated by the peak pattern presented in Figure 4. By comparing to the JCPDS database[13], hexagonal InN should have the highest intensity for (101), which is not present in the spectrum (Fig. 4) instead the highest intensity is for the (002) peak, indicating that the film growth has a preferred orientation of (002).[14]

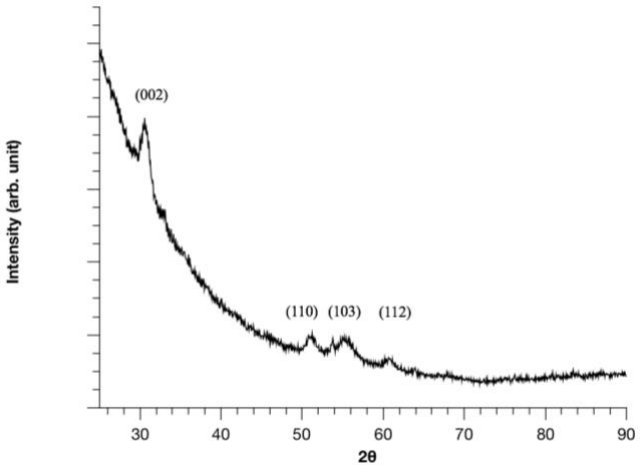

FIG. 4. GIXRD showing polycrystalline hexagonal InN deposited with 5 s pulse of **1**.

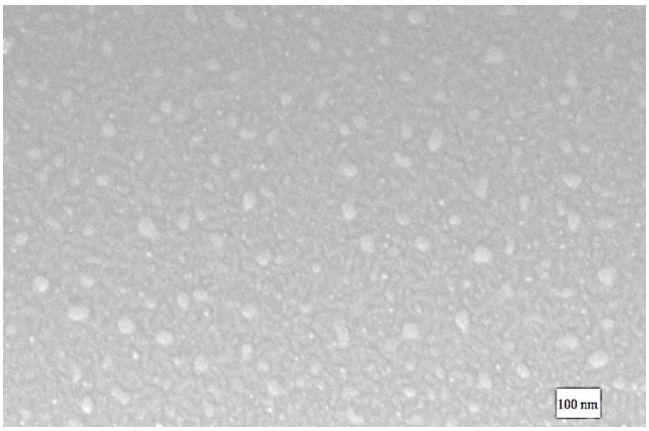

FIG. 5. Top view SEM micrograph showing the morphology of the InN film deposited with a 5 s pulse of **1**.

Top view SEM (Fig. 5) shows that the film is composed of many small crystalline grains with a significant size variation; smaller grains are indicative of a nucleation points that formed later in the deposition, while other "older" features are larger. This difference in size is an indication that the film grows in an island growth manner with continuous re-nucleation. The chemical environment of the deposited films was analysed by XPS, but due to the low thickness of the films it was difficult to undertake depth profiling and to sputter-clean the surface. The XPS measurement revealed that the oxygen and carbon

impurities are present on the film surface to a level of 18.3 at. % and 20.1 at. %, respectively; this is not unexpected as the grown films were exposed to air for some days before XPS analysis. Sputter cleaning of the film surface could not be performed due to the low film thickness. As the films are polycrystalline, some diffusion of oxygen and carbon dioxide further down into the film via grain boundary diffusion, is also expected.[15]

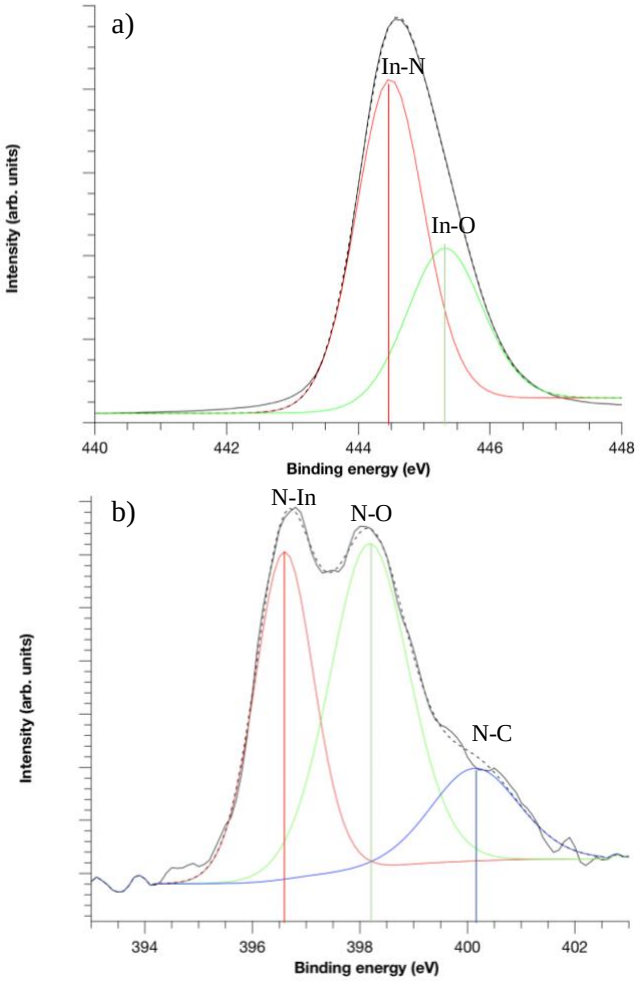

FIG. 6. High resolution XPS scan of a) In $3d_{5/2}$ and b) N 1s. In $3d_{5/2}$ were fitted for In-N and In-O from left to right, respectively, and N 1s were fitted for N-In, N-O and N-C from left to right, respectively.

Figure 6a shows the high resolution XPS scan for In $3d_{5/2}$; two sub-peaks were found to produce a good fit for the spectrum where the peaks at 444.4 eV and 445.3 eV were assigned to the In-N bond and In-O bond, respectively. These results correlate well with previous XPS studies of InN.[16, 17, 18] The shift between the In-N and the In-O core levels were found to be 0.9 eV. Previous studies found this shift to be approximately 1 eV.[16, 17] Figure 6b shows the N 1s high resolution scan with three sub-peaks revealed by curve-fitting. The three subpeaks at 396.6, 398.2 and 400.1 eV were assigned to N-In, N-O bond and N-C bond, respectively.[16, 17, 18] The presence of N-C bonds is attributed to remaining guanidinate ligands on the surface. The In-N bond was observed in both the In $3d_{5/2}$ and N 1s high resolution XPS spectra, thus confirming the GIXRD result that the films are InN.

Attempts to deposit thicker films by increasing the number of ALD cycles failed due to the instability of **1** in the heated bubbler. New batches of precursor were used for each deposition experiment, but the decomposition of **1** left about half of initial weight in the bubbler as a grey powder after each run. The fill-empty pulsing scheme, required to move **1** from the bubbler into the deposition chamber, added a significant amount of time to each ALD cycle. Thus, increasing the number of ALD cycles led to long deposition times and decomposition of a large portion of the precursor into a grey powder. The remaining powder was extracted by C_6D_6 and the supernatant was analysed by ^{1}H NMR , however, it appeared that only a small portion of the powder dissolved which indicates that **1** decomposes mostly into insoluble products in the bubbler. The ^{1}H NMR spectrum of the dissolved powder (Fig. S4) showed the same, unidentified thermolysis product as previously reported.[19] The possibility to only do a low number of ALD cycles together

with a possible nucleation delay of InN on Si are seen as the main reasons for the low growth rates found in this study.

IV. SUMMARY AND CONCLUSIONS

Tris-*N*,*N*-dimethyl-*N*',*N*''-diisopropylguanidinatoindium(III) (**1**) was used as a In precursor together with NH_3 plasma in a time-resolved CVD process to deposit InN films. Approximately 10 nm hexagonal InN thin films where deposited with about 0.1 nm/cycle, a preferred (002) orientation and high levels of oxygen and carbon on the surface. The carbon and oxygen impurities are believed to be caused by air exposure prior to characterization. The poor thermal stability of **1** in the bubbler at 160 °C made it difficult to grow thicker films and fully characterize the deposition process. While we show in this study that **1** can be used as an In precursor, its poor thermal stability makes it a poorly suited precursor for InN.

ACKNOWLEDGMENTS

This project was founded by the Swedish foundation for Strategic Research through the project "Time-resolved low temperature CVD for III-nitrides" (SSF-RMA 15-0018) and by the Knut and Alice Wallenberg foundation through the project "Bridging the THz-gap" (KAW 2013.0049). HP acknowledges the Wenner-Gren foundations and the COST Action MP1402 'Hooking together European research in atomic layer deposition (HERALD) supported by COST (European Cooperation in Science and Technology) for funding for a sabbatical at Carleton University. STB and SCB acknowledge the Vinnova VINNMER Marie Curie incoming mobility program for funding for a sabbatical and research visits to Linköping University (Vinnova grant 2015-03714). HP and STB are

very grateful for the networking support provided from the COST Action HERALD. Jason Coyle is acknowledged for fruitful discussions. XPS of the precipitate and films deposited with N_2 plasma by David Mandia is gratefully acknowledged.

[1] A. G. Bhuiyan, A. Hashimoto, and A. Yamamoto, J. Appl. Phys **94**, 2779–2808 (2003).

[2] E. Bellotti, B. K. Doshi, K. F. Brennan, J. D. Albrecht, and P. P. Ruden, J. Appl. Phys. **85**, 916–923 (1999).

[3] K. S. A. Butcher and T. L. Tansley, Superlattices Microstruct. **38**, 1–37 (2005).

[4] S. V. Ivanov, T. V. Shubina, T. A. Komissarova and V. N. Jmerik, J. Cryst. Growth **403**, 83-89 (2014).

[5] S. Ruffenach, M. Moret, O. Briot and B. Gil, Phys. Stat. Sol. A **207**, 9-18 (2010).

[6] K. Rönnby, S. C. Buttera, P. Rouf, S. T. Barry, L. Ojamäe and H. Pedersen, Methylamines as Nitrogen Precursors in Chemical Vapor Deposition of Gallium Nitride. ChemRxiv. Preprint. (2018). DOI: 10.26434/chemrxiv.7067687.v1

[7] N. Nepal, N. A. Mahadik, L. O. Nyakiti, S. B. Qadri, M. J. Mehl, J. K. Hite, and C. R. Eddy, Cryst. Growth Des. **13**, 1485-1490 (2013).

[8] A. Haider, S. Kizir and N. Biyikli, AIP Advances **6**, 045203 (2016).

[9] S. C. Buttera, D. J. Mandia, S. T. Barry, J. Vac. Sci. Technol. A **35**, 01B128 (2017).

[10] S. C. Buttera, K. Rönnby, H. Pedersen, L. Ojamäe and S.T. Barry J. Vac. Sci. Technol. A **36**, 01A101 (2018).

[11] P. G. Gordon, M. J. Ward, M. J. Heikkila, W. H. Monillas, G. P. A. Yap, M. Ritala, M. Leskalä, S. T. Barry, Dalton Trans. **40**, 9425-9430 (2011).

[12] M. Gebhard, M. Hellwig, H. Parala, K. Xu, M. Winter, A. Devi, Dalton Trans. **43**, 937-940 (2014).

[13] Joint Committee on Powder Diffraction Standards, JCPDS, Swarthmore, PA, pattern: 00-050-1239.

[14] W. Paszkowicz , J. Adamczyk , S. Krukowski , M. Leszczyński , S. Porowski , J. A. Sokolowski , M. Michalec and W. Łasocha, Philos. Mag. A **79**, 1145-1154 (1999).

[15] William. D. Callister, *Materials Science and Engineering*, SI Version, John Wiley & Sons Ltd. 8th edition (ISBN: 978-0-470-50586-1)

[16] T. D. Veal, P. D. C. King, P. H. Jefferson, L. F. J. Piper, C. F. McConville, Hai Lu, W. J. Schaff, P. A. Anderson, S. M. Durbin, D. Muto, H. Naoi and Y. Nanishi, Phys. Rev. B **76**, 075313 (2007).

[17] C.L Wu, H.M. Lee, C. T. Kuo, C. H. Chen and S. Gwo, Phys. Rev. Lett.,**101**, 106803 (2008).

[18] T. Nagata, G. Koblmüller, O. Bierwagen, C. S. Gallinat and J. S. Speck, Appl. Phys. Lett., **95**, 132104 (2009).

[19] M. Gebhard, M. Hellwig, H. Parala, K. Xu, M. Winter and A. Devi, Dalton Trans., **43**, 937 (2014).